



King Saud University
Arabian Journal of Chemistry

www.ksu.edu.sa
www.sciencedirect.com



ORIGINAL ARTICLE

Ozone catalytic oxidation of toluene over 13X zeolite supported metal oxides and the effect of moisture on the catalytic process

T. Gopi, G. Swetha, S. Chandra Shekar *, R. Krishna, C. Ramakrishna, Bijendra Saini, P.V.L. Rao

Defence R&D Establishment, Jhansi Road, Gwalior, MP 474002, India

Received 13 March 2016; revised 26 July 2016; accepted 27 July 2016

KEYWORDS

13X zeolite;
Ozone;
Catalytic oxidation;
Toluene;
Moisture

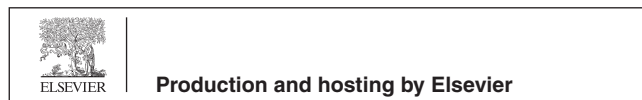
Abstract This paper reports the behavior of 13X zeolite supported Ce, Cu, Co, Ag and Mn metal oxides toward ozone catalytic oxidation (OZCO) of toluene and the influence of moisture on the decomposition process. The simple impregnation method was adapted to disperse the metal oxides and found highly active for toluene oxidation in the presence of ozone. The steady-state activities and ozone decomposition data reveal that the activity is in the order of Mn/13X > Ce/13X > Cu/13X > Ag/13X > Co/13X and Mn/13X > Cu/13X > Ce/13X > Ag/13X > Co/13X, respectively. The extent of ozone decomposition is responsible for the degree of oxidative decomposition of toluene over the Mn/13X catalyst. The addition of moisture (Relative Humidity of 25%) to the reaction mixture considerably enhanced the conversion of toluene and selectivity to carbon oxides from 49% to 61% and 38% to 53% respectively, on the Mn/13X catalyst. The two sets of experiment results reveal that the surface adsorbed by-products such as benzene, benzaldehyde, p-methyl phenol and oxalic acid are considerably oxidized to CO₂ in the presence of moisture whereas in the absence of moisture these by-products are slowly oxidized. The activity data in the presence of ozone and moisture also reveal that the moisture has considerably enhanced the activation of surface adsorbed by-products than that of initial toluene oxidation. Based on the temperature programmed desorption and temperature programmed oxidation studies, the addition of moisture decreased the by-products accumulation thereby, reduced the catalyst deactivation and enhanced the extended oxidation of toluene on the Mn/13X zeolite.

© 2016 The Authors. Production and hosting by Elsevier B.V. on behalf of King Saud University. This is an open access article under the CC BY-NC-ND license (<http://creativecommons.org/licenses/by-nc-nd/4.0/>).

* Corresponding author. Fax: +91 7103 280610.

E-mail address: sridarac@yahoo.com (S.C. Shekar).

Peer review under responsibility of King Saud University.



1. Introduction

Volatile organic compounds (VOCs) are the major contributor to air pollution due to their toxic and fusty nature, concern in global warming, smog formation, etc. Many industrial processes and transportation activities lead to the accumulation of VOCs in the atmosphere (Bastos et al., 2012), and hence control of VOCs is the key challenge

<http://dx.doi.org/10.1016/j.arabjc.2016.07.018>

1878-5352 © 2016 The Authors. Production and hosting by Elsevier B.V. on behalf of King Saud University.

This is an open access article under the CC BY-NC-ND license (<http://creativecommons.org/licenses/by-nc-nd/4.0/>).

Please cite this article in press as: Gopi, T. et al., Ozone catalytic oxidation of toluene over 13X zeolite supported metal oxides and the effect of moisture on the catalytic process. Arabian Journal of Chemistry (2016), <http://dx.doi.org/10.1016/j.arabjc.2016.07.018>

within the research area of environmental catalysis. Several methods are employed for the removal of VOCs, including thermal/catalytic oxidation, plasma-catalysis, biological degradation, photo catalysis and adsorption processes (Huang et al., 2015; Wu and Wang, 2014). Among these methods, catalytic oxidation is the promising process for the removal of VOCs, which converts the harmful VOCs into harmless CO₂ and H₂O (Liotta et al., 2013; Wu and Wang, 2011; Wu et al., 2011a, 2011b). In the recent years, ozone catalytic oxidation (OZCO) has gained much attention for the oxidation of VOCs due to the strong oxidizing ability of ozone (Einaga et al., 2013). It is also reported that the ozone has significantly decreased the process temperature, and the activation energy compared to that catalytic oxidation with molecular oxygen (Shekar et al., 2011).

Several studies described the use of transition metal oxides for ozone catalytic oxidation of VOCs (Mehandjiev et al., 2001). Einaga and co-workers examined the activity of alumina supported transition metal oxides and observed that the Mn/Al₂O₃ catalyst is the most active for the benzene oxidation and ozone decomposition whereas the Co/Al₂O₃ is more active for alone ozone decomposition (Einaga and Futamura, 2004). It is opined that the higher surface area supports, and lower manganese loadings are favorable to enhance the ozone assisted benzene oxidation due to the high dispersion over the support (Einaga and Ogata, 2009; Einaga et al., 2009). Several reports focused on high surface area supports such as ZSM-5, MCM-41, SBA-15 and 13X zeolite for OZCO of VOCs (Huang et al., 2015; Jin et al., 2013; Rezaei and Soltan, 2012; Chao et al., 2007). Sugasawa and Ogata investigated the activity of ZSM-5 supported transition metal oxides for the catalytic oxidation of toluene and it is observed that manganese catalyst is more active for toluene conversion, whereas silver catalyst is selective toward carbon dioxide (Sugasawa and Ogata, 2011). Rezaei and Soltan reported the Mn/Al₂O₃ is more active than that of Mn/MCM-41 for the catalytic ozonation of toluene under identical manganese loading though the MCM-41 has considerable surface area (Rezaei and Soltan, 2012). In contrast, Einaga et al. reported the SiO₂ supported manganese oxides with high surface area are the better catalysts for ozonation of VOCs in terms of the activity and efficient ozone utilization (Einaga et al., 2014). On the other hand, alone 13X zeolite also employed for the removal of trace amount of toluene by OZCO and 90% of toluene is effectively oxidized to carbon oxides (Chao et al., 2007). Li et al. reported that the high toluene activity in the presence of ozone due to the presence of oxygen vacancies presented on the surface of the catalyst and observed higher activity over Mn–Ag/HZSM-5 (Li et al., 2014). However, Long et al. reported that the high ozone concentrations played a major role in the complete oxidation of toluene by accelerating the surface adsorbed acid group by-products to CO₂ (Long et al., 2011).

Though the OZCO was recognized as an effective method for VOCs oxidation at the low temperatures, it also suffers from several challenges related to the applicability of the process to practical application. One of the biggest challenges is the deactivation of catalysts at the ambient temperatures due to the accumulation of organic by-products such as weakly bound formic acid and strongly bound surface formate and carboxylates (Huang et al., 2015; Einaga and Futamura, 2006). Although some attempts have been made to enhance the VOCs oxidation and prevent the deactivation of the catalyst such as catalyst heating is one of the methods frequently used to overcome this problem (Rezaei and Soltan, 2012). In contrast, the addition of water vapor also reported to alter the catalytic activity and suppress the catalyst deactivation to some extent (Einaga and Futamura, 2006; Liu et al., 2014). However, the reported studies on the catalytic activity of transition metal oxides and the effect of moisture in the process of OZCO are still debatable for practical applications. It is also important to identify the exact reasons whether moisture is increasing the oxidation capacity of ozone or suppressing the by-products adsorption by maintaining the clean surface during the ozone catalytic reaction, which is one of the key factors for the catalyst stability and long-term operations.

The metal nature, metal dispersion and nature of support and its surface area are playing an important role in the ozone catalytic oxidation of VOCs and ozone decomposition (Reed et al., 2005; Jin et al., 2011). The 13X zeolite is well cited in the literature for high surface area for the dispersion of metal oxides besides its stability in ozone catalytic oxidations (Chao et al., 2007). Hence, the 13X zeolite supported Mn, Ag, Co, Cu and Ce oxides are prepared by impregnation method and elucidated for the ozone catalytic oxidation of toluene, and the optimum catalyst is investigated for the effect of moisture in the presence of ozone. Based on these studies, the effect of moisture on the carbon oxides selectivity and by-products activation is also summarized.

2. Material and methods

2.1. Preparation of catalysts

The 13X zeolite (M/s. Sorbed India, sieved to 18/25 BSS mesh) supported Ce, Cu, Co, Ag and Mn catalysts are synthesized by incipient wet impregnation. In order to impregnate the Ce, Cu, Co, Ag and Mn the Ce(NO₃)₃·6H₂O, Cu(NO₃)₂·3H₂O, Co(NO₃)₂·6H₂O (Aldrich, 99%), AgNO₃ (Aldrich, 99.5%) and Mn(NO₃)₂·2H₂O (Aldrich, 99%) salts were used as precursors respectively. The requisite amounts (1.43 mmol Ce(NO₃)₃·6H₂O, 3.14 mmol Cu(NO₃)₂·3H₂O, 3.39 mmol of Co(NO₃)₂·6H₂O, 1.85 mmol AgNO₃ and 3.63 mmol Mn(NO₃)₂·2H₂O) of metal precursors were dissolved in 50 mL of distilled water to get 2 wt% metal. Thereafter, the precursor solution was added to the 13X support (9.8 g) and stirred for 2 h at 40 °C and the removal of excess water and cobalt nitrate decomposition was performed simultaneously by the microwave irradiation using the 300 W for 15 min with manual stirring for a frequency of 3 min. The purpose of the microwave decomposition of metal nitrates is rapid decomposition of metal salts over the 13X zeolite to minimize the nucleation of the metal oxides (Wang et al., 2015). As the heat-transfer coefficient and microwave interaction of 13X zeolite is relatively lower to that of cobalt nitrate (Ionic in nature). Hence intrinsic temperatures are considerably higher for the cobalt nitrate (Bilecka and Niederberger, 2010). The microwave dried catalysts were further calcined at 550 °C by passing the cylinder air of 100 mL/min for 6 h and are denoted as Ce/13X, Cu/13X, Co/13X, Ag/13X and Mn/13X.

2.2. Characterization of catalysts

The BET specific surface area and pore size distribution of the calcined catalysts were determined with a Micromeritics, ASAP2020 instrument using nitrogen adsorption at –196 °C. The specific surface areas of the samples were calculated with the multi-point Brunauer-Emmett-Teller (BET) procedure and micropore size distributions determined with Horváth-Kawazoe (HK) method.

X-ray diffraction (XRD) patterns of the catalysts were recorded on a shimadzu, X-ray diffractometer using Ni filtered Cu K α radiation ($\lambda = 1.5406 \text{ \AA}$) in a scan range of 10–80°.

The temperature programmed reduction (TPR) was carried out on a TPR unit (Nuchrom Technologies, India) using 100 mg of catalyst under 50 mL/min gas flow of hydrogen (5%) in argon. Before the analysis, catalyst was preheated in helium flow of 50 mL/min at 400 °C for 2 h. The consumption of hydrogen (reduction) profile was recorded by raising the

temperature from 50 °C to 730 °C at rate of heating 10 °C/min using a thermal conductivity detector (TCD).

The TEM images of the catalysts were obtained on a high-resolution transmission electron microscope (HR-TEM JEOL 2010 LaB6) at an acceleration voltage and point resolution of 200 kV and 0.19 nm respectively. Prior to the analysis, a tiny amount of sample was dispersed in ethanol using ultrasonic bath and then deposited on carbon coated 200 mesh copper grid.

The infrared spectra of prepared catalysts were recorded in the range of 400–4000 cm^{-1} on a Perkin Elmer Spectrum 65 spectrometer with a resolution of 4 cm^{-1} . Samples were diluted with potassium bromide (KBr) and palletized before analysis.

2.3. Catalytic activity studies

2.3.1. Reaction setup

Catalytic activity experiments were carried out in a continuous flow, fixed-bed quartz reactor at an atmospheric pressure and the detailed procedure was described elsewhere (Shekar et al., 2011). The reactor was loaded with 400 mg of catalyst (18/25 BSS mesh sieved) between two quartz wool plugs, and it was mounted vertically in an electrically heated tubular furnace (Carbolite, USA) which is displayed in Fig. 1. Prior to the reaction, the catalyst was activated at 200 °C in the oxygen flow for an hour. Gas phase toluene was generated by injecting the liquid toluene (Aldrich 99.9%) with an infusion pump (Cole Parmer, USA) into the heating chamber (at 120 °C), at a rate of 0.25 mL/h and supplemented by the carrier gas of dry air 750 mL/min (Alchemie gases, India). The standardized ozone generator (Eltech engineers, India) was used to generate the ozone by passing the dry oxygen (250 mL/min, 99.9% Alchemie gases, India) with a precise mass flow controller (Sierra instruments, The Netherlands) and was directly introduced to the catalyst bed to minimize the gas phase reactions (Soni et al., 2015). The un-reacted ozone was scrubbed with KI solution after the ozone analyzer. The generated concentrations of toluene and ozone were 890 and 7650 ppmv, respectively. Moisture content was maintained by passing the air through a water bubbler thermo-stated at 40 °C and the relative humidity (RH) of the reaction mixture was measured with a hygrometer (Fisher scientific, China).

The quantitative analysis of the reaction products was carried out by passing the gas stream into an online Gas Chromatograph equipped with Flame Ionization Detector (Bruker GC) having an HP-5 capillary column (30 m \times 0.25 mm). The qualitative analysis of the products was done by GC-MS (Agilent 6890N, USA) using identical column. The carbon oxides and un-reacted ozone were analyzed with CO (SR 94 electrochemical based detectors, ranging from 1 to 2000 ppmv), CO₂ (IR based detectors P90 M/s. Technovation Analytical Instruments Ltd., India, ranging over 10–20,000 ppmv) and ozone analyzers (M/s. Eltech Eng. India, range 0–200 N g/m³), respectively.

2.3.2. Tracking the moisture effect on the surface of the catalyst during the reaction

In order to track the influence of moisture content on the OZCO of toluene, two sets of experiments were performed. In the first experiment, the oxidation of toluene with ozone was performed under identical conditions for an hour at 90 °C using the 400 mg of catalyst. Further, the toluene and ozone feed was stopped and the catalyst was flushed with air for five minutes to remove the weakly bound surface by-products. The simple ozonation reaction was performed on the used catalyst in the absence of toluene gas under comparable conditions, and the effluents were analyzed by the CO, CO₂ analyzers. In the second set of experiment, the catalyst (400 mg) was saturated with toluene vapor under identical conditions without using the ozone gas for an hour and in similar way the catalyst was treated and the ozone gas was passed without any toluene feed. Both the sets of experiments were repeated at two different moisture contents (RH = 0.1 and 25%).

2.3.3. TPD and TPO of by-products analysis by online GC-MS

Temperature programmed desorption (TPD) and temperature programmed oxidation (TPO) experiments were performed for the used catalysts to quantify the by-products adsorbed during reaction. The Helium (purity: 99.99%) and dry air (21% O₂) were employed as carrier gases for the TPD and TPO studies, respectively. The catalyst (100 mg of used) was taken in a quartz reactor and it was heated from 30 to 630 °C at a rate of heating 8 °C/min under a carrier gas flow. The effluent

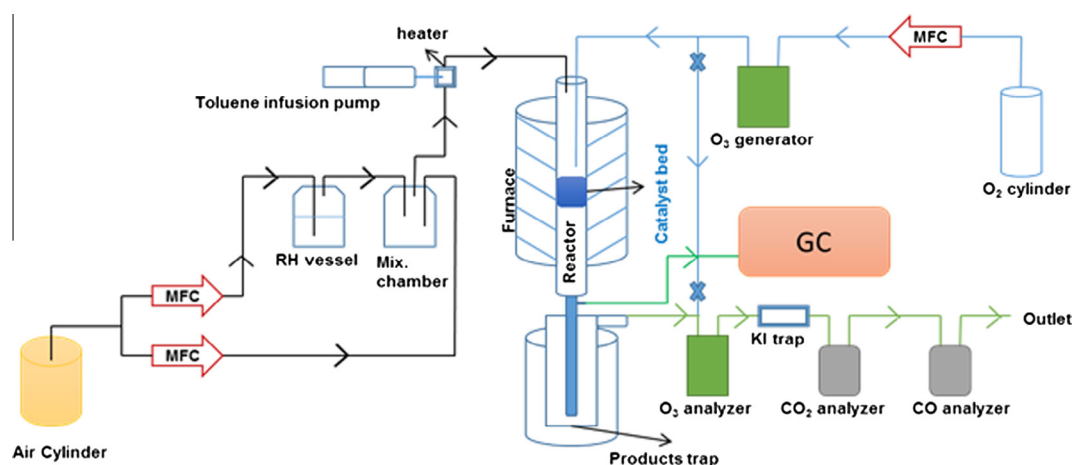


Figure 1 A schematic experimental setup.

gas stream was analyzed with an online GC-MS and CO, CO₂ analyzers.

3. Results and discussion

3.1. HR-TEM analysis

The metal oxide dispersion was determined by the high resolution transmission electron microscope (HR-TEM), and the micrographs are displayed in Fig. 2. The images reveal that the good light contrast crystalline phase morphology is observed and ascribed to the host 13X zeolite. On the other hand, the dark contrast of high electron density particles is attributed to the dispersed metal oxides, and these particles are observed for Ce/13X, Ag/13X and Cu/13X catalysts (Taghavi-moghaddam et al., 2012). In contrast, on the Mn/13X and Co/13X catalysts, the dark particles are not observed in TEM analysis. It appears that manganese and cobalt oxides are highly dispersed state and hence the particles are not observed in the TEM images which may be due to the formation of particles below the TEM detection limit. However, it is evident as of the Energy Dispersive X-ray (EDS)

spectrum the respective metal content for cobalt and manganese metal is 3.03 and 2.43 wt%.

From the TEM analysis and the literature reports, the observed particles of Ce/13X, Ag/13X and Cu/13X catalysts were assigned for the respective metal oxides (Garcia et al., 2013; Masui et al., 2003; Conte et al., 2012). The CeO₂ and Ag₂O particles are in the range of 2–7 nm size, whereas CuO particles are in the range of 10–25 nm and all the metal oxides represented the crystalline nature. From the results, it can conclude that all the metal oxides are finely dispersed on the 13X zeolite.

3.2. XRD studies

The X-ray diffraction patterns of 13X zeolite and supported catalysts are shown in Fig. 3. The results revealed that all the catalysts exhibited the diffraction signals at $2\theta = 10, 11.6, 15.4, 20, 23.3, 26.7, 29.3$ and 31 which correspond to the typical pattern of crystalline 13X zeolite (Ma et al., 2014). The XRD profiles of all catalysts showed similar diffraction lines to those of bare 13X zeolite, which indicate the structural framework is retained even after incorporation

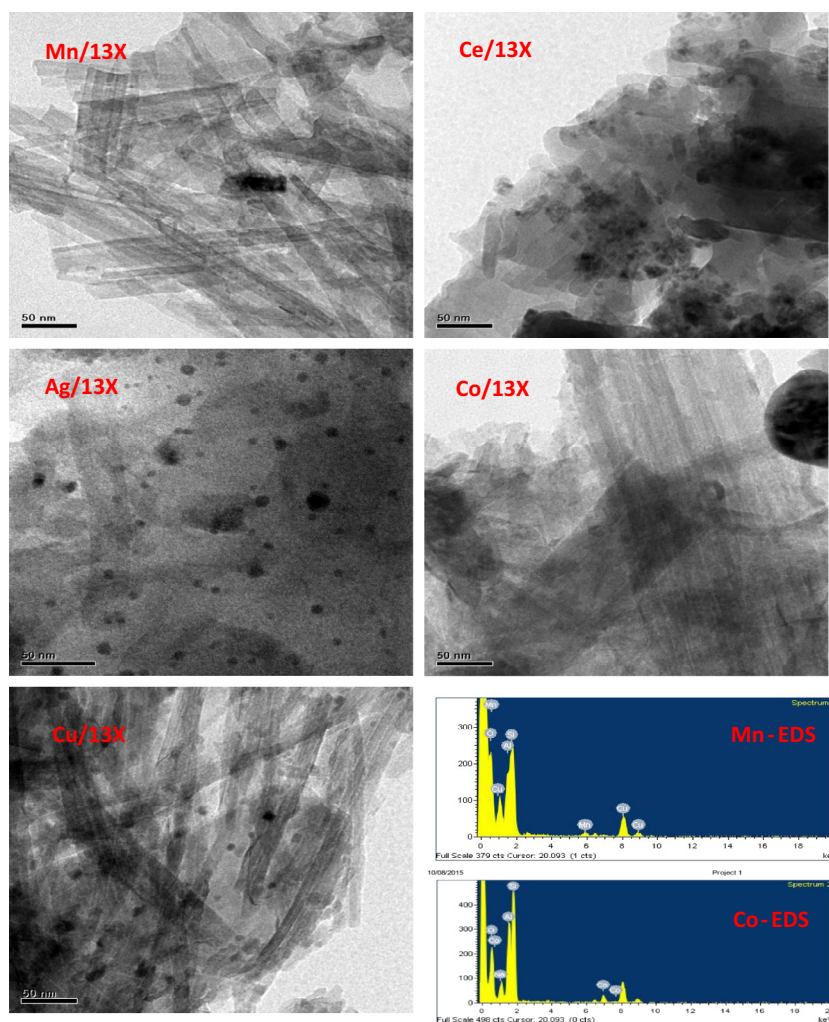


Figure 2 TEM images of calcined catalysts.

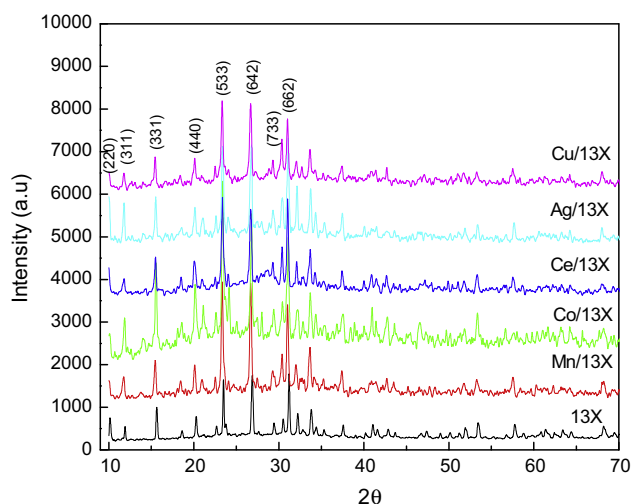


Figure 3 XRD patterns of calcined 13X, Mn/13X, Co/13X, Ce/13X, Ag/13X and Cu/13X catalysts.

of metal oxides. However, no significant metal oxide peaks are found in the profiles of all the catalysts, which may be attributed to the uniform dispersion of metal oxides on 13X zeolite, as observed by TEM in Fig. 2. It is obvious that the metal oxide particles present in the catalysts are below the XRD detection limits. The similar reports are observed on ZSM-5 and SiO₂ supported MnO_x (Huang et al., 2015; Einaga and Ogata, 2009).

3.3. BET surface area analysis

The N₂ adsorption-desorption isotherms and pore size distributions of 13X zeolite and impregnated catalysts are displayed in Fig. 4. The results reveal that the N₂ adsorption-desorption isotherms of impregnated catalysts are similar to the support 13X zeolite (Fig. 4a). The sharp rise in adsorption isotherms in the low relative pressure region (0.001–0.1 p/p^o) indicates that the catalysts contain microporous structure (Du and Wu, 2007). However, the amount of adsorbed N₂ is decreased with the impregnation of metal, which is due to the blockage of the pores, especially at the micropores (Sánchez et al., 2016). It can be observed from Table 1 that, the micropore surface area and micropore volumes of all the impregnated catalysts are decreased from the support 13X zeolite, whereas the external surface area is almost constant. The reductions in the surface area and pore volumes are moderate for Mn/13X, Co/13X, Ce/13X and Ag/13X catalysts. In contrast, for Cu/13X catalyst the reduction in surface area is significant which, is due to the formation of relatively larger CuO particles on the surface of the support which is apparent in the TEM analysis.

3.4. Temperature programmed reduction studies

In order to ascertain the reducibility of dispersed metal oxides on the support 13X zeolite, temperature programmed reduction (TPR) experiments were performed for the support as well as the catalysts and the results are shown in Fig. 5. The Cu/13X, Ag/13X and Ce/13X catalysts are shown a single reduced peak centered at 294, 188 and 648 °C which is assigned

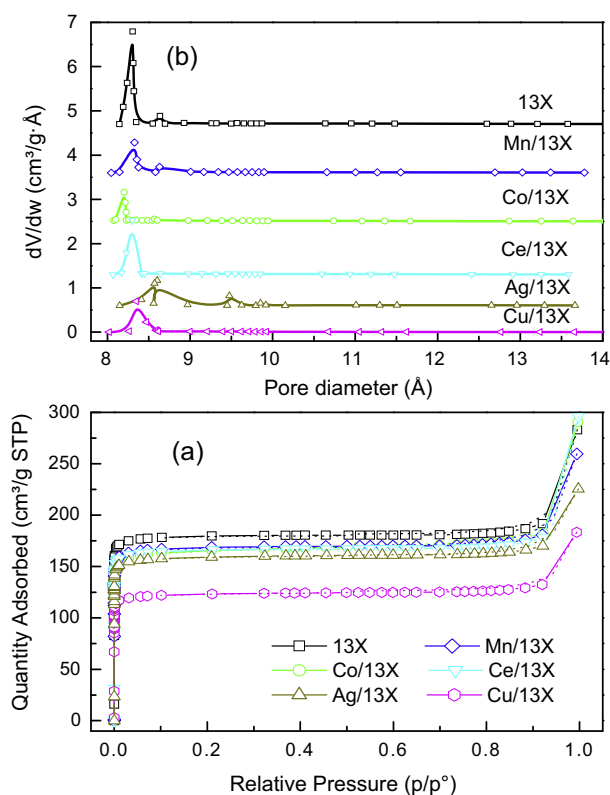


Figure 4 (a) N₂ adsorption-desorption isotherms and (b) pore size distributions of calcined 13X, Mn/13X, Co/13X, Ce/13X, Ag/13X and Cu/13X catalysts.

to the reduction of CuO to Cu, Ag₂O to Ag and CeO₂ to Ce, respectively (Poreddy et al., 2015; Li et al., 2014; Konsolakis et al., 2015; Wu et al., 2014). These symmetric reduction peaks demonstrate that the Cu, Ag and Ce metal oxides are homogeneously dispersed on 13X zeolite. On the other hand, Mn/13X and Co/13X catalyst showed multistep reduction peaks centered at 350, 490 °C and 490, 612 °C, respectively. The two-step reduction on the Mn/13X catalyst is ascribed to the reduction of Mn₂O₃ to Mn₃O₄, and Mn₃O₄ to MnO (Poreddy et al., 2015; Li et al., 2014). The low-temperature reduction peak in the Co/13X catalyst ascribed to the Co₂O₃ to CoO and the high-temperature peak is assigned to the CoO to metallic Co (Konsolakis et al., 2015). It appears that Cu, Ag and Ce oxides are in the single oxidation state which could be Cu²⁺, Ag¹⁺ and Ce⁴⁺ whereas multiple oxidation states for Mn and Co metal oxides are present in the catalyst such as Mn²⁺, Mn³⁺, Co²⁺ and Co³⁺. The results are well correlated with the reported literature of supported and unsupported metal oxides (Poreddy et al., 2015; Li et al., 2014; Konsolakis et al., 2015).

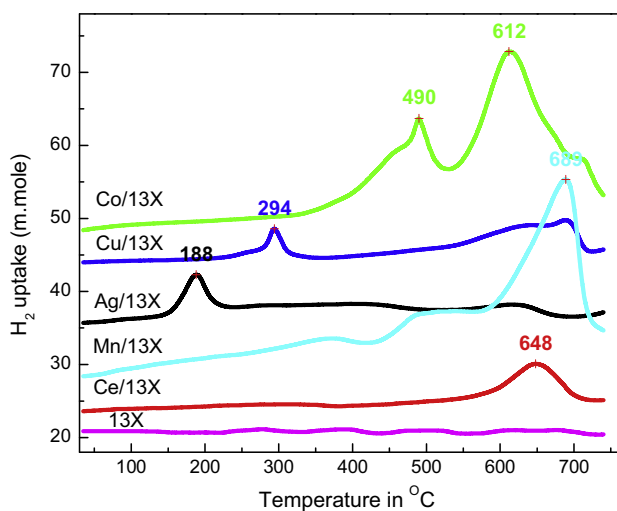
4. Activity studies

4.1. Comparison studies of toluene OZCO on various 13X zeolite supported metal oxides

The catalytic activities of toluene oxidation with ozone on various catalysts were evaluated for 100 min and the results are

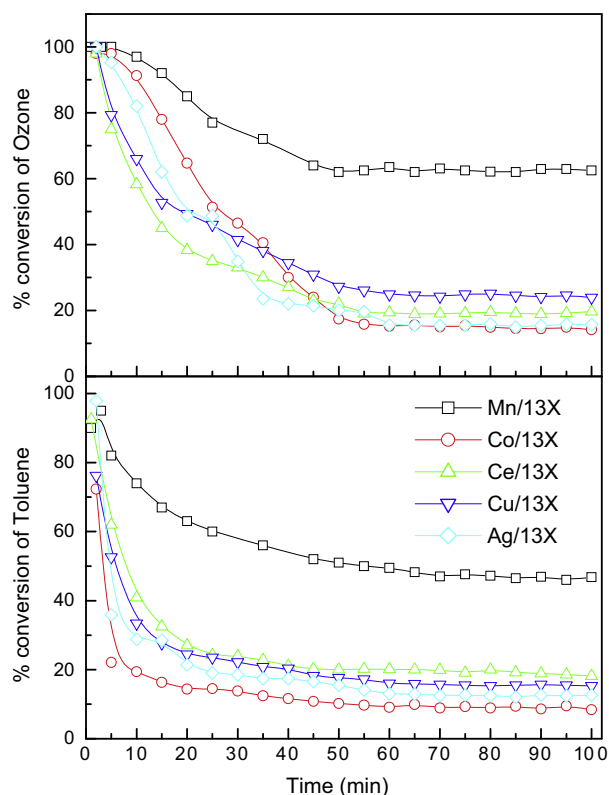
Table 1 Physical characteristics of 13X zeolite and impregnated catalysts.

Catalyst	BET surface area (m ² /g)	Micropore surface area (m ² /g)	External surface area (m ² /g)	Micropore volume (cm ³ /g)	% Metal from SEM-EDAX
13X	746	716	30	0.264	–
Mn/13X	684	648	35	0.245	2.6
Co/13X	665	612	53	0.232	3.9
Ce/13X	679	648	31	0.243	3.7
Cu/13X	449	422	27	0.140	9.1
Ag/13X	656	622	34	0.231	3.6

**Figure 5** TPR profiles of calcined 13X, Mn/13X, Co/13X, Ce/13X, Ag/13X and Cu/13X catalysts.

shown in Fig. 6. The process parameters were maintained at temperature of 90 °C, toluene feed concentration of 896 ppmv and the ozone concentration of 7650 ppmv. The % conversions of toluene and ozone after 100 min are summarized in Table 2. The selectivity to CO and CO₂ is calculated based on the amount of CO₂ formed, divided by that of toluene reacted for OZCO of toluene (Table 2).

The results reveal that all the catalysts are active for the oxidation of toluene in the presence of ozone and the toluene conversion values (Fig. 6) are decreased with time on stream and reached to a steady state value after 50 min for all the catalysts. However, the reduction in the conversion values is minimum in case of Mn/13X catalyst, whereas decrease is more pronounced for Co/13X, Ce/13X, Cu/13X and Ag/13X catalysts. The toluene oxidation and ozone decomposition follow the similar tendencies with respect to the time on stream analysis. It appears that the extent of toluene oxidation is function of ozone decomposition under employed conditions. However, the molar ratio between ozone to toluene reacted for all the catalysts is in the range of 10–15. It appears that the ozone decomposition plays a significant role in the toluene oxidation and high ozone catalytic decomposition catalysts are offering the better toluene conversions (Einaga and Ogata, 2010). On the other hand, the Ag/13X catalyst shows significant selectivity (71%) to CO₂, and the similar results are reported by Einaga and Ogata on the Ag/Al₂O₃ for the benzene oxidation in the presence of ozone (Einaga and Ogata, 2010). The Mn/13X and Ce/13X catalysts also exhibited considerable

**Figure 6** Change in the conversions of toluene and ozone with time on Mn/13X, Co/13X, Ce/13X, Ag/13X and Cu/13X catalysts. Conditions: catalyst 400 mg, toluene 896 ppmv, ozone 7650 ppmv, reaction temp 90 °C.

selectivity to CO₂ (67.5% and 62.5%), whereas the selectivity to CO₂ is quite lower for the Cu/13X and Co/13X catalysts. From the results it can conclude that, the Cu/13X and Co/13X catalysts have less selectivity to CO₂ with lower conversion levels whereas Ce/13X and Ag/13X catalysts have high selectivity to CO₂ with comparable conversions. On the other hand, the Mn/13X catalyst is highly selective to CO₂ with high degree of toluene conversion.

As it is evident from the activity data for the Mn/13X catalyst, the better toluene and ozone conversions are observed at 90 °C. The significant activity of manganese oxide is in line with the literature reports for toluene oxidation in the presence of ozone over alumina supported manganese catalyst (Rezaei et al., 2013). The better activity over the Mn/13X catalyst is due to the high ozone decomposition capacity of manganese oxides presented on the surface of the support (Einaga et al.,

Table 2 Catalytic activities for toluene oxidation with ozone.^a

Catalyst	% Toluene conversion	% Ozone conversion	Rate, $\times 10^{-5}$ mol g ⁻¹ min ⁻¹		Ratio ^b	% Selectivity ^c	
			Toluene	Ozone		CO ₂	CO
13X	2.0	3.2	0.19	2.73	14.48	16.1	8.1
Mn/13X	46.8	62.5	4.41	53.33	12.09	67.5	9.2
Co/13X	8.4	14.1	0.79	12.03	15.20	35.5	7.1
Ce/13X	18.2	19.6	1.72	16.72	9.75	62.8	8.9
Cu/13X	15.3	23.9	1.44	20.39	14.14	27.6	1.8
Ag/13X	12.6	15.7	1.19	13.40	11.28	71.3	4.7

^a Catalyst 400 mg, toluene 896 ppmv, ozone 7650 ppmv, reaction temperature 90 °C. The data are obtained after 100 min.

^b Ratio is calculated based on the moles of ozone consumed divided by that of the moles of toluene converted.

^c Selectivity is calculated based on the amount of CO₂ formed divided by that of toluene reacted.

2009). It also reported that the O₃ is decomposed to O₂ on supported manganese oxide catalysts according to the steps described in Eqs. (1)–(3), where * refers to the catalytic active sites of manganese oxide (Huang et al., 2015; Dhandapani and Oyama, 1997). The active oxygen species (O* and O₂*) formed on the catalyst surface by ozone decomposition are responsible for the toluene oxidation.



It is noteworthy in mentioning that the catalytic activity of Mn/13X offers high selectivity to CO₂ (67.5%) compared to that of Mn/Al₂O₃ (22%) with comparable conversions (Einaga and Ogata, 2010), which is an added advantage of Mn/13X catalyst for industrial effluent stream process. Hence further studies are focused on the Mn/13X catalyst for detailed analysis.

In order to understand the variations in the catalytic process performance at an ambient reaction temperature and time on stream data, the used catalysts are subjected to infrared spectroscopy. For the sake of comparison, the calcined catalysts were analyzed with FT-IR and the results are depicted in Fig. 7b. From the results, infrared spectra of fresh catalysts show a peak at 1635 cm⁻¹ and a broad peak from 3100 to 3500 cm⁻¹, are ascribed to the bending vibrations of adsorbed water and the hydroxyl groups present on the catalysts, respectively. On the other hand, the infrared spectra of used catalysts (Fig. 7a) show additional peaks at 1410, 1565, 1715 and 2945 cm⁻¹, are referred to symmetric and asymmetric COO⁻ stretching vibration of esters, C=O stretching vibration of acids/aldehydes and symmetric C–H stretching vibration of CH₃ groups, respectively (Ma et al., 2014; Long et al., 2011). The FTIR data of used catalysts clearly demonstrate that the considerable reaction by-products retain on the surface of the catalysts during the reactions which lead to the catalyst deactivation.

4.2. Effect of reaction temperature

The effect of temperature on toluene, ozone conversions, and CO_x formation on the Mn/13X catalyst was elucidated, and the results are depicted in Fig. 8. Initially, the reaction was car-

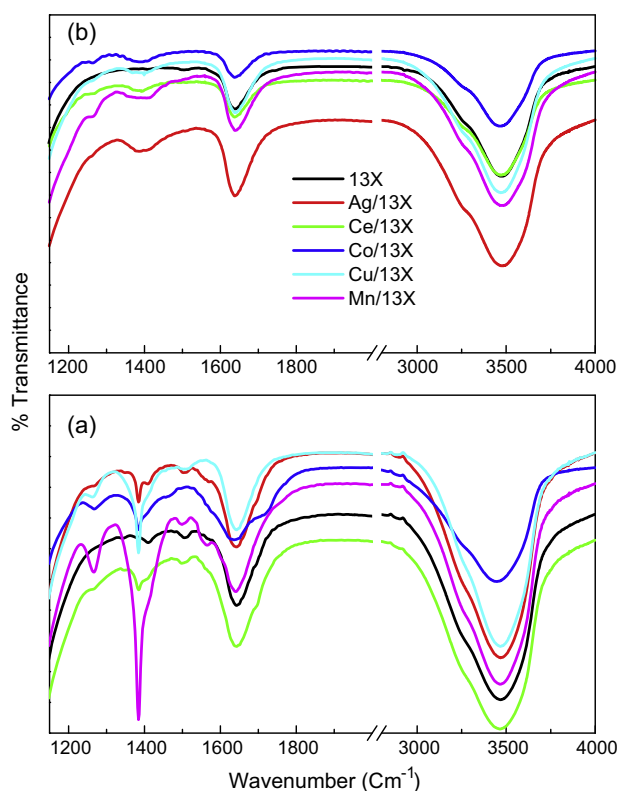


Figure 7 FT-IR spectra of the (a) deactivated and (b) fresh catalysts after 100 min reaction at 90 °C.

ried out at 30 °C till to attain the steady state, which was approximately 60 min, and then the reaction temperature was raised to 60, 90, 120 and 150 °C and allowed to stabilize for 30 min at each temperature. The results reveal that the toluene and ozone conversions are steadily increased with temperature and attained the maximum conversions at 150 °C. In contrast, the molar ratio of ozone to toluene converted is increased from 9.5 to 10.1 with temperature, which is due to the acceleration of thermal decomposition of ozone as well as utilization of ozone to the toluene oxidation with the temperature. It is noteworthy in mentioning that the ratio of ozone to toluene decomposition gives a measure for the relative influence of reaction temperature on the OZCO. It appears that

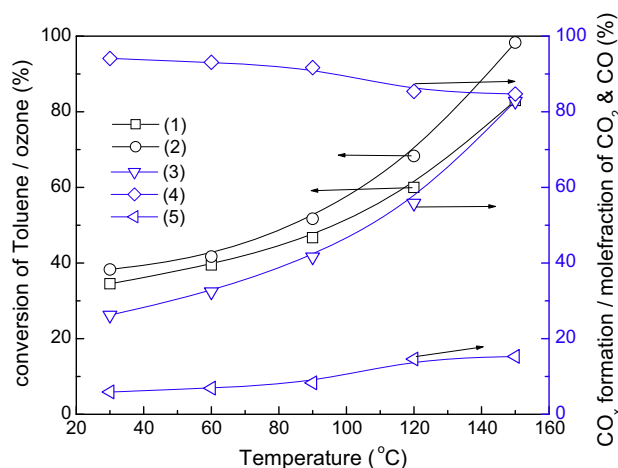


Figure 8 Toluene, ozone conversions and CO_x formation as a function of reaction temperature. (1) Toluene conversion, (2) ozone conversion, (3) CO_x formation, (4) mole fraction of CO_2 , (5) mole fraction of CO . Conditions: catalyst 400 mg, toluene 896 ppmv, ozone 7650 ppmv.

with increasing the reaction temperature the slight thermal decomposition is facilitated compared to that of toluene activation. The carbon oxide (Eq. (4)) formation is also increased with temperature; however, the variation in mole fraction of CO and CO_2 is marginal.

$$\% \text{CO}_x = \frac{\text{CO}_x \text{ concentration in ppmv}}{(\text{toluene inlet concentration in ppmv} \times 7)} \times 100 \quad (4)$$

These results demonstrate that, though the ozone is strong oxidizer at the low-temperature, the minimum reaction temperature of 80–100 °C is essential to mineralize the toluene completely to carbon oxides over the Mn/13X catalyst in the presence of ozone. Hence, further the reaction studies are performed at a reaction temperature of 90 °C.

4.3. Effect of moisture on OZCO of toluene

The effect of moisture on the toluene oxidation, ozone decomposition and CO_x formation on the Mn/13X catalyst was elucidated, and the results are depicted in Fig. 9 with increasing the moisture content, toluene and ozone conversions and CO_x formations go through a maximum at a RH of 25–30%. At above 30% RH, the toluene and ozone conversions are decreased, which might be due to the competitive adsorption between moisture and reactants. Overall, RH of 25–30% is optimum for the better toluene conversions and CO_x formations under employed conditions on Mn/13X catalyst.

Further, the long-term activity studies at above optimized RH% were performed and results such as toluene oxidation, ozone decomposition and mole fractions of CO , CO_2 on the Mn/13X catalyst are depicted in Fig. 10. From the results, the toluene conversions are sharply decreased in the absence of moisture (Fig. 10a) to 49.5% at 60 min, which is due to the deactivation of catalysts by strong adsorption of by-products. In contrast, the conversions are steadily decreased in the presence of moisture (Fig. 10b) reached to a steady value of 61% at 60 min.

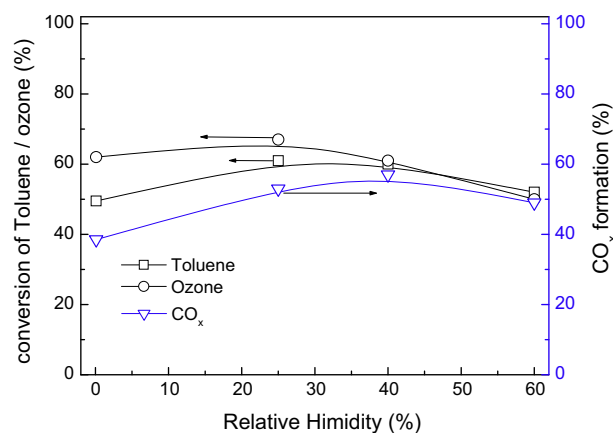


Figure 9 Toluene, ozone conversions and CO_x formation as a function of Relative Humidity.

The mole ratio of ozone to the toluene conversion is decreased from 12 to 9.5, when the moisture is employed. These results indicate that the toluene conversions are accelerated in the presence of moisture and the decomposed ozone is efficiently utilized for the toluene oxidation for the moisture used condition. The CO_x formations and CO_2 mole fractions are also significantly higher in the presence of moisture and

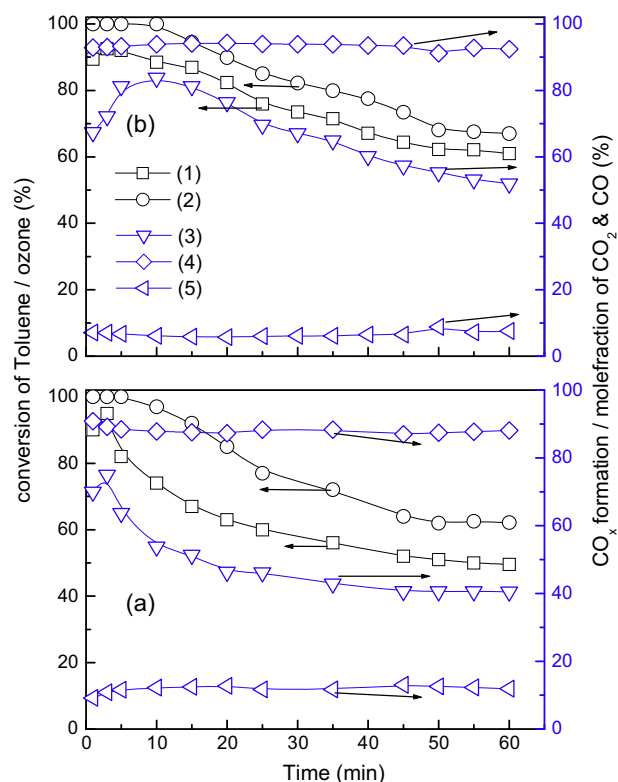


Figure 10 Toluene, ozone conversions and CO_x formation as a function of time. (a) In dry air (RH of 0.1%), (b) in the presence of moisture (RH of 25%), (1) toluene conversion, (2) ozone conversion, (3) CO_x formation, (4) mole fraction of CO_2 , (5) mole fraction of CO . conditions: catalyst 400 mg, toluene 896 ppmv, ozone 7650 ppmv.

ozone. The oxygen species (O^*) formed in catalytic ozonation reaction may convert the surface adsorbed moisture to the hydroxyl radicals (OH^*) which are more active species for the oxidation of toluene besides promoting the oxidation of strongly surface bound by-products (Huang et al., 2015; Einaga and Futamura, 2006; Zhao et al., 2012).



Hence, the addition of moisture to the reaction stream considerably enhanced the toluene conversion to CO_2 . The carbon oxide formation as function of toluene consumption (Fig. 11) reveals the quantitative toluene consumption and the corresponding CO_x formation in the presence of moisture is very close to the 100% compared to that of in the absence of moisture, which clearly demonstrates that the complete mineralization of toluene to CO_x is enhanced besides oxidation of adsorbed by-products on the surface of the catalyst.

4.4. Tracking the moisture effect on the surface of the catalyst during the reaction

In order to track the influence of moisture content on the OZCO of toluene, two sets of experiments were performed. In the first experiment, the oxidation of toluene with ozone was performed under identical conditions for an hour at 90 °C using the 400 mg of catalyst and further the toluene and ozone feed was stopped and the catalyst was flushed with air for five minutes to remove the weakly bound surface by-products. The simple ozonation reaction was performed on the used catalyst without employing the toluene gas under comparable conditions and the effluents were analyzed by the CO, CO_2 analysers. In the second experiment, the catalyst (400 mg) saturated with toluene vapor under identical conditions without using the ozone gas for an hour and similar

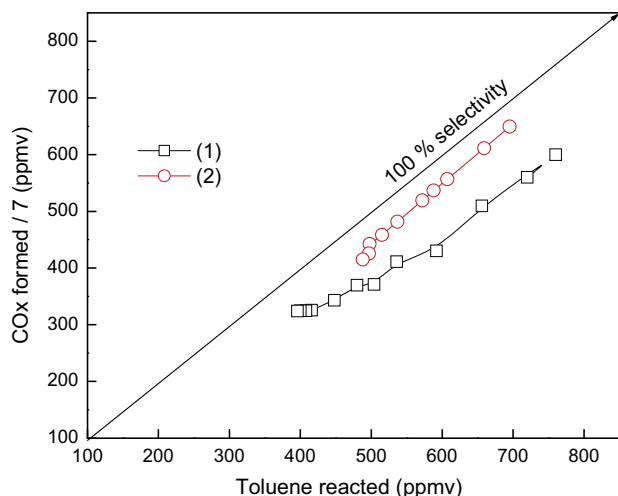


Figure 11 Relationship between the toluene consumption and CO_x formation (carbon balance) on Mn/13X catalyst, (1) in the absence of moisture, (2) in the presence of moisture (RH of 25%), conditions: catalyst 400 mg, toluene 896 ppmv, ozone 7650 ppmv.

way the catalyst was treated and ozone gas was passed without any toluene feed. Both the set of experiments were repeated at two different moisture content (RH = 0.1% and 25%).

The first set of experimental results (Fig. 12a) reveals that, by-products on the catalyst surface are oxidized to CO_x when ozone is introduced in the absence of toluene and the elution of CO_x was observed for more than 60 min. It is noteworthy in mentioning that (Fig. 12a) the CO_x concentrations significantly enhanced in the presence of moisture compared than those in the absence of moisture. The elution of CO_x is quite faster and the complete surface adsorbed by-products converted to CO_x in the presence of moisture. From these results, it is obvious that significant increase in the by-products oxidation is attributed to the reaction of ozone with moisture in producing the strong oxidizing species such as OH radicals that in turn responsible for high oxidation rates (Huang et al., 2015). It appears that addition of moisture greatly enhanced the catalytic activity and stability of the catalyst by reducing the catalyst deactivation for the Mn/13X catalyst at the ambient temperatures.

In second set of experimental results (Fig. 12b) it is revealed that when the ozone introduced over toluene adsorbed catalyst, initially the CO_x formation is almost similar for 15 min in the presence and absence of moisture. However, the CO_x formation is increased for 30 min and almost CO_x formation disappeared after 60 min in the presence of moisture; in contrast, the CO_x formation is drastically reduced in the absence of moisture to 150 ppmv and the continuous elution is observed for longer time. It appears that initially, the toluene is oxidized to CO_x besides forming some by-products on the

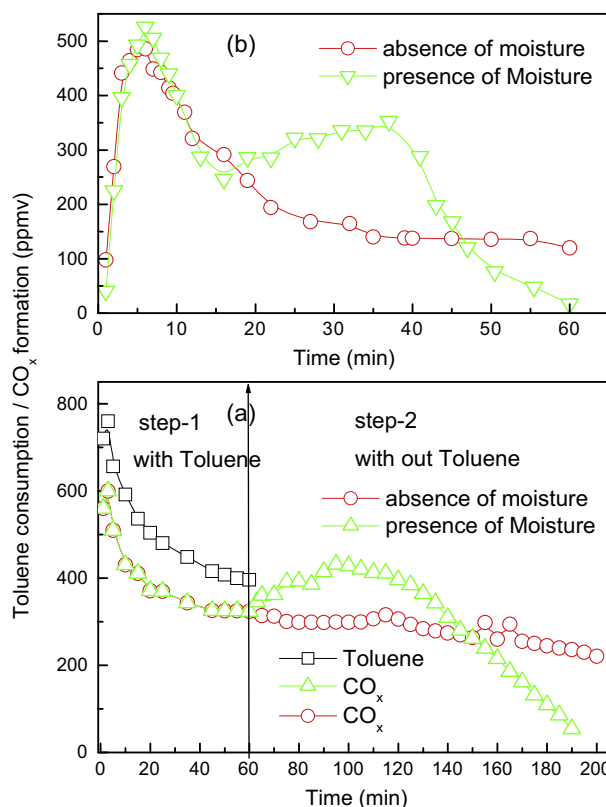


Figure 12 Effect of moisture (a) on the by-products activation and (b) on the toluene initial oxidation.

surface of the catalyst. The formed by-products are oxidized slowly to CO_x and may be retained on the surface even after two hours in the absence of moisture.

The results of second set of experiment also confirm with the first set of experiments, which clearly indicate that the effect of moisture on initial toluene oxidation is nearly negligible, and further the moisture increased the CO_x formation by oxidizing the adsorbed by-products much faster in the presence of moisture.

4.5. TPD and TPO studies of Mn/13X used catalysts for by-products analysis

To ascertain the accumulation of by-products on the surface of the catalyst the used catalysts in both the conditions (in the presence of moisture and in the absence of moisture) were subjected to the TPD experiments using helium as a carrier in the temperature range of 30–600 °C. The desorbed products were analyzed by online GC-MS, and the results are displayed in Fig. 13. From the results, it is clearly visible the desorption of used catalysts in the absence and presence of moisture exhibited the similar low temperature (from 30 to 300 °C) and a high temperature (from 300 to 600 °C) patterns. However, the amount of desorbed products from the used catalysts in the presence of moisture is less than that of the used catalysts in the absence of moisture.

The qualitative results obtained on the effluent stream of TPD analysis of the used catalyst in the absence of moisture

indicate the toluene is eluted as the major product and benzaldehyde, and oxalic acid observed as minor products at the low temperature region, whereas, toluene, benzaldehyde, para methyl phenol, and benzoic acid are eluted as minor products and benzene is the major product at the high-temperature region. On the other hand, the effluent stream analyses of used catalyst in the presence of moisture, toluene, oxalic acid and acetic acid are eluted at the low-temperature region, whereas benzene and benzaldehyde are eluted at high temperature with relatively low abundance of all the observed products compared to that of in the absence of moisture. These results inferred that the by-products accumulation significantly decreased in the presence of moisture under in OZCO.

Temperature programmed oxidation (TPO) experiments were conducted to identify the residual species present on the used Mn/13X catalyst surface under oxidative environment, and results are displayed in Fig. 14. The CO_2 elution for the used catalyst (in the absence of moisture) is observed in two temperature regions where the elution at low temperature (T_{max} of 260 °C) region corresponded to the oxidation of weakly bound surface by-products on the catalyst, which are identified in TPD experiment as toluene and oxalic acid. On the other hand, the CO_2 evolution at high temperature (T_{max} of 390 °C) region ascribed to the oxidation of strongly bound by-products such as benzene, benzaldehyde, para methyl phenol and benzoic acid (see Fig. 15).

On the other hand, it is interested to observe the TPO of used catalyst (in the presence of moisture) is shown only one low temperature CO_2 evolution peak at a T_{max} of 260 °C to that of in the absence of moisture. Thus, the moisture has significantly reduced the build-up of by-products on the catalyst surface and oxidized the by-products at relatively lower temperatures. The TPO results also confirm that the significant by-products are deposited on the surface of the catalysts during the OZCO of toluene at low-temperature, which are responsible for the catalyst deactivation, and it is considerably minimized in the presence of moisture. The results are in line with the observations of Einaga and Ogata reported for the benzene oxidation over alumina supported silver catalyst (Einaga and Ogata, 2010).

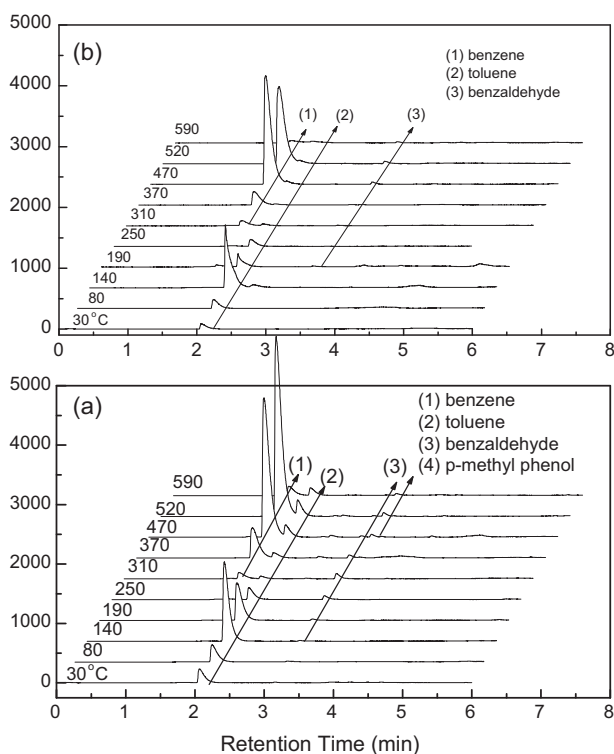


Figure 13 TPD profile; Total ion chromatograms of by-products desorption as a function of temperature for used Mn/13X catalyst (a) in the absence of moisture and (b) in the presence of moisture. Conditions: catalyst 100 mg, He carrier 100 mL/min, rate of heating 8 °C/min.

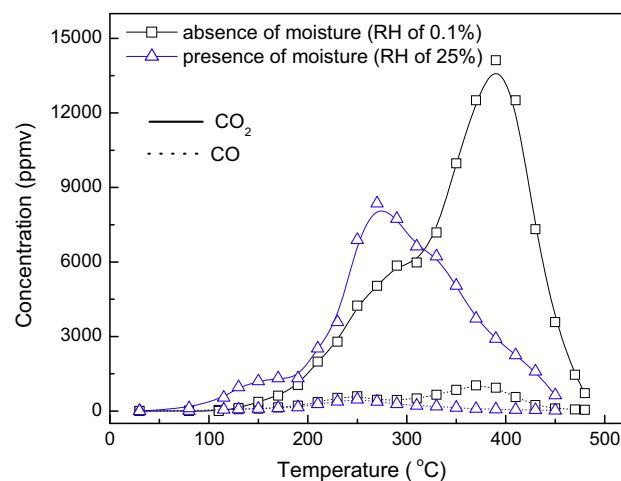


Figure 14 TPO profile of used Mn/13X catalyst (a) in the absence of moisture and (b) in the presence of moisture. Conditions: catalyst 100 mg, air flow 200 mL/min, rate of heating 8 °C/min.

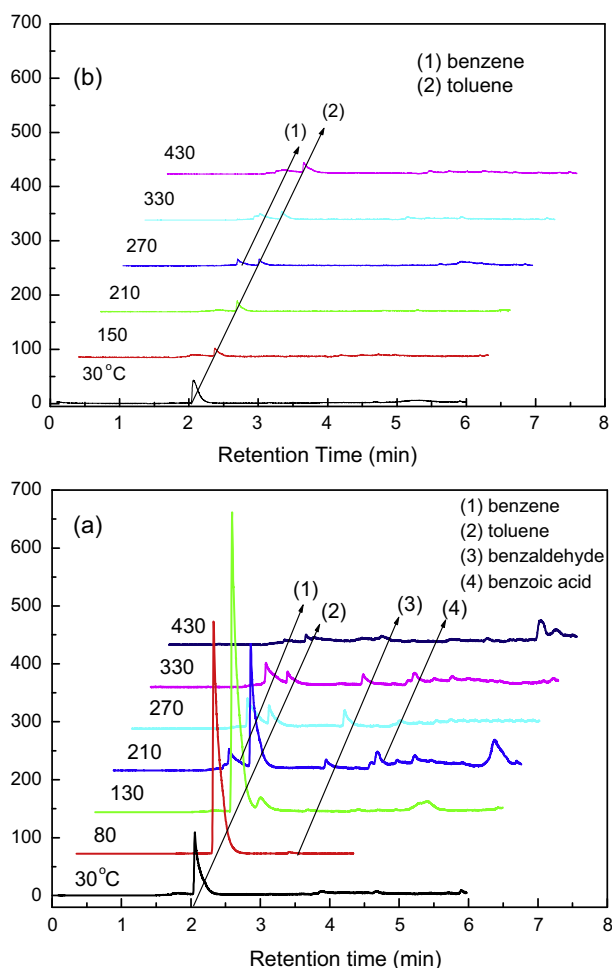


Figure 15 Total ion chromatograms of by-products desorption during the TPO analysis for used Mn/13X catalyst (a) in the absence of moisture and (b) in the presence of moisture.

5. Conclusion

13X zeolite supported Ce, Cu, Co, Ag and Mn metal oxides are prepared and characterized by BET-SA, XRD, TEM and TPR. These results reveal that the metal oxides are well dispersed on the high surface 13X zeolite support by simple impregnation. The Mn and Co catalysts are finely dispersed compared to those of Ag, Ce, and Cu catalysts. The prepared catalysts are elucidated for OZCO of toluene, and all the catalysts are active for the toluene oxidation with varying the conversion values from 10% to 50% with selectivity to carbon oxides. It is interesting to note that the manganese oxides over 13X is identified as better ozone and toluene conversions with considerable selectivity to CO_2 among all the catalysts. The effect of reaction temperature and moisture results on the Mn/13X catalyst results reveals slightly higher temperatures are favorable for the deep oxidation of toluene to CO_x and the moisture greatly enhances the toluene conversion and selectivity to CO_2 at ambient temperatures. The molar ratio of ozone to toluene consumption is also decreased from 12 to 9.5 with the addition of moisture implies that the amount of ozone required to the oxidative decomposition to CO_2 can be significantly reduced by addition of moisture to the reaction stream. The effect of moisture experiments on the used catalyst results proved that the addition of moisture increased the oxidation of surface adsorbed by-products compared to the initial activation of toluene. On the other hand, the TPD and TPO results also demonstrated that, the presence of moisture

in the reaction stream decreased the by-products accumulation and enhanced the oxidation capacity. Therefore, the moisture greatly decreased the catalyst deactivation and increased the stability with higher selectivity to CO_2 on the Mn/13X zeolite.

Acknowledgments

One of the authors T. Gopi is grateful to Council of Scientific and Industrial Research, New Delhi, India, for awarding the fellowship. The authors are also obliged to the Dr. A.K. Gupta, A.P. Bansod and Director, DRDE for the necessary support to carry out the research work. The authors are grateful to Dr. K.S. Ramarao, Dr. G.K. Prasad and Dr. K. Kadirvelu for providing the X-ray diffraction, BET-surface area and SEM-EDAX analysis.

References

- Bastos, S.S.T., Carabineiro, S.A.C., Órfão, J.J.M., Pereira, M.F.R., Delgado, J.J., Figueiredo, J.L., 2012. Total oxidation of ethyl acetate, ethanol and toluene catalyzed by exotemplated manganese and cerium oxides loaded with gold. *Catal. Today* 180, 148–154.
- Bilecka, I., Niederberger, M., 2010. Microwave chemistry for inorganic nanomaterials synthesis. *Nanoscale* 2, 1358.
- Chao, C.Y.H., Kwong, C.W., Hui, K.S., 2007. Potential use of a combined ozone and zeolite system for gaseous toluene elimination. *J. Hazard. Mater.* 143, 118–127.
- Conte, M., Lopez-Sanchez, J.A., He, Q., Morgan, D.J., Ryabenkova, Y., Bartley, J.K., Carley, A.F., Taylor, S.H., Kiely, C.J., Khalid, K., Hutchings, G.J., 2012. Modified zeolite ZSM-5 for the methanol to aromatics reaction. *Catal. Sci. Technol.* 2, 105–112.
- Dhandapani, B., Oyama, S.T., 1997. Gas phase ozone decomposition catalysts. *Appl. Catal. B Environ.* 11, 129–166.
- Du, X., Wu, E., 2007. Porosity of microporous zeolites A, X and ZSM-5 studied by small angle X-ray scattering and nitrogen adsorption. *J. Phys. Chem. Solids* 68, 1692–1699.
- Einaga, H., Futamura, S., 2006. Effect of water vapor on catalytic oxidation of benzene with ozone on alumina-supported manganese oxides. *J. Catal.* 243, 446–450.
- Einaga, H., Futamura, S., 2004. Comparative study on the catalytic activities of alumina-supported metal oxides for oxidation of benzene and cyclohexane with ozone. *React. Kinet. Catal. Lett.* 81, 121–128.
- Einaga, H., Harada, M., Ogata, A., 2009. Relationship between the structure of manganese oxides on alumina and catalytic activities for benzene oxidation with ozone. *Catal. Lett.* 129, 422–427.
- Einaga, H., Ogata, A., 2010. Catalytic oxidation of benzene in the gas phase over alumina-supported silver catalysts. *Environ. Sci. Technol.* 44, 2612–2617.
- Einaga, H., Ogata, A., 2009. Benzene oxidation with ozone over supported manganese oxide catalysts: effect of catalyst support and reaction conditions. *J. Hazard. Mater.* 164, 1236–1241.
- Einaga, H., Teraoka, Y., Ogata, A., 2013. Catalytic oxidation of benzene by ozone over manganese oxides supported on USY zeolite. *J. Catal.* 305, 227–237.
- Einaga, H., Yamamoto, S., Maeda, N., Teraoka, Y., 2014. Structural analysis of manganese oxides supported on SiO_2 for benzene oxidation with ozone. *Catal. Today* 242, 2–7.
- Garcia, T., Sellick, D., Varela, F., Vázquez, I., Dejoz, A., Agouram, S., Taylor, S.H., Solsona, B., 2013. Total oxidation of naphthalene using bulk manganese oxide catalysts. *Appl. Catal. A Gen.* 450, 169–177.
- Huang, H., Ye, X., Huang, W., Chen, J., Xu, Y., Wu, M., Shao, Q., Peng, Z., Ou, G., Shi, J., Feng, X., Feng, Q., Huang, H., Hu, P., Leung, D.Y.C., 2015. Ozone-catalytic oxidation of gaseous benzene

- over MnO₂/ZSM-5 at ambient temperature: catalytic deactivation and its suppression. *Chem. Eng. J.* 264, 24–31.
- Jin, M., Lu, P., Yu, G.X., Cheng, Z.M., Chen, L.F., Wang, J.A., 2013. Effect of additives doping on catalytic properties of Mg₃(VO₄)₂ catalysts in oxidative dehydrogenation of cyclohexane. *Catal. Today* 212, 142–148.
- Jin, M., Wook, J., Man, J., Jurng, J., Bae, G., Jeon, J., Park, Y., 2011. Effect of calcination temperature on the oxidation of benzene with ozone at low temperature over mesoporous α -Mn₂O₃. *Powder Technol.* 214, 458–462.
- Konsolakis, M., Sgourakis, M., Carabineiro, S.A.C., 2015. Surface and redox properties of cobalt–ceria binary oxides: on the effect of Co content and pretreatment conditions. *Appl. Surf. Sci.* 341, 48–54.
- Li, J., Na, H., Zeng, X., Zhu, T., Liu, Z., 2014. In situ DRIFTS investigation for the oxidation of toluene by ozone over Mn/HZSM-5, Ag/HZSM-5 and Mn–Ag/HZSM-5 catalysts. *Appl. Surf. Sci.* 311, 690–696.
- Liotta, L.F., Wu, H., Pantaleo, G., Venezia, A.M., 2013. Co₃O₄ nanocrystals and Co₃O₄-MO_x binary oxides for CO, CH₄ and VOC oxidation at low temperatures: a review. *Catal. Sci. Technol.* 3, 3085–3102.
- Liu, Y., Li, X., Liu, J., Shi, C., Zhu, A., 2014. Ozone catalytic oxidation of benzene over AgMn/HZSM-5 catalysts at room temperature: effects of Mn loading and water content. *Chin. J. Catal.* 35, 1465–1474.
- Long, L., Zhao, J., Yang, L., Fu, M., Wu, J., Huang, B., Ye, D., 2011. Room temperature catalytic ozonation of toluene over MnO₂/Al₂O₃. *Chin. J. Catal.* 32, 904–916.
- Ma, Y., Yan, C., Alshameri, A., Qiu, X., Zhou, C., Li, D., 2014. Synthesis and characterization of 13X zeolite from low-grade natural kaolin. *Adv. Powder Technol.* 25, 495–499.
- Masui, T., Hirai, H., Hamada, R., Imanaka, N., Adachi, G., Sakata, T., Mori, H., 2003. Synthesis and characterization of cerium oxide nanoparticles coated with turbostratic boron nitride. *J. Mater. Chem.* 13, 622–627.
- Mehandjiev, D., Naydenov, A., Ivanov, G., 2001. Ozone decomposition, benzene and CO oxidation over NiMnO₃-ilmenite and NiMn₂O₄-spinel catalysts. *Appl. Catal. A Gen.* 206, 13–18.
- Poreddy, R., Engelbrekt, C., Riisager, A., 2015. Copper oxide as efficient catalyst for oxidative dehydrogenation of alcohols with air. *Catal. Sci. Technol.* 5, 2467–2477.
- Reed, C., Xi, Y., Oyama, S.T., 2005. Distinguishing between reaction intermediates and spectators: a kinetic study of acetone oxidation using ozone on a silica-supported manganese oxide catalyst. *J. Catal.* 235, 378–392.
- Rezaei, E., Soltan, J., 2012. Low temperature oxidation of toluene by ozone over MnO_x/ γ -alumina and MnO_x/MCM-41 catalysts. *Chem. Eng. J.* 198–199, 482–490.
- Rezaei, E., Soltan, J., Chen, N., 2013. Catalytic oxidation of toluene by ozone over alumina supported manganese oxides: effect of catalyst loading. *Appl. Catal. B Environ.* 136–137, 239–247.
- Sánchez, G., Dlugogorski, B.Z., Kennedy, E.M., Stockenhuber, M., 2016. Zeolite-supported iron catalysts for allyl alcohol synthesis from glycerol. *Appl. Catal. A Gen.* 509, 130–142.
- Shekar, S. Chandra, Soni, K., Bunkar, R., Sharma, M., Singh, B., Suryanarayana, M.V.S., Vijayaraghavan, R., 2011. Vapor phase catalytic degradation of bis(2-chloroethyl) ether on supported vanadia–titania catalyst. *Appl. Catal. B Environ.* 103, 11–20.
- Soni, K.C., Shekar, S.C., Singh, B., Gopi, T., 2015. Catalytic activity of Fe/ZrO₂ nanoparticles for dimethyl sulfide oxidation. *J. Colloid Interface Sci.* 446, 226–236.
- Sugasawa, M., Ogata, A., 2011. Effect of different combinations of metal and zeolite on ozone-assisted catalysis for toluene removal. *Ozone Sci. Eng.* 33, 158–163.
- Taghavimoghaddam, J., Knowles, G.P., Chaffee, A.L., 2012. Preparation and characterization of mesoporous silica supported cobalt oxide as a catalyst for the oxidation of cyclohexanol. *J. Mol. Catal. A: Chem.* 358, 79–88.
- Wang, N., Qiu, J., Wu, Z., Wu, J., You, K., Luo, H., 2015. Effect of microwave calcination on catalytic properties of Pt/MgAl(Sn)O_x catalyst in cyclohexane dehydrogenation to cyclohexene. *Appl. Catal. A Gen.* 503, 62–68.
- Wu, H., Pantaleo, G., La Parola, V., Venezia, A.M., Collard, X., Aprile, C., Liotta, L.F., 2014. Bi- and trimetallic Ni catalysts over Al₂O₃ and Al₂O₃-MO_x (M = Ce or Mg) oxides for methane dry reforming: Au and Pt additive effects. *Appl. Catal. B Environ.* 156, 350–361.
- Wu, H., Wang, L., 2014. Phase transformation-induced crystal plane effect of iron oxide micropine dendrites on gaseous toluene photocatalytic oxidation. *Appl. Surf. Sci.* 288, 398–404. <http://dx.doi.org/10.1016/j.apsusc.2013.10.046>.
- Wu, H., Wang, L., 2011. Shape effect of microstructured CeO₂ with various morphologies on CO catalytic oxidation. *Catal. Commun.* <http://dx.doi.org/10.1016/j.catcom.2011.05.018>.
- Wu, H., Wang, L., Shen, Z., Zhao, J., 2011a. Catalytic oxidation of toluene and p-xylene using gold supported on Co₃O₄ catalyst prepared by colloidal precipitation method. *J. Mol. Catal. A: Chem.* 351, 188–195. <http://dx.doi.org/10.1016/j.molcata.2011.10.005>.
- Wu, H., Wang, L., Zhang, J., Shen, Z., Zhao, J., 2011b. Catalytic oxidation of benzene, toluene and p-xylene over colloidal gold supported on zinc oxide catalyst. *Catal. Commun.* 12, 859–865.
- Zhao, D.Z., Shi, C., Li, X.S., Zhu, A.M., Jang, B.W.L., 2012. Enhanced effect of water vapor on complete oxidation of formaldehyde in air with ozone over MnO_x catalysts at room temperature. *J. Hazard. Mater.* 239–240, 362–369.